

Measurement of the cross section for $e^+e^- \rightarrow \Xi^-\bar{\Xi}^+$ and observation of an excited Ξ baryon

M. Ablikim¹, M. N. Achasov^{10,d}, P. Adlarson⁵⁹, S. Ahmed¹⁵, M. Albrecht⁴, M. Alekseev^{58A,58C}, A. Amoroso^{58A,58C}, F. F. An¹, Q. An^{55,43}, Y. Bai⁴², O. Bakina²⁷, R. Baldini Ferroli^{23A}, I. Balossino^{24A}, Y. Ban^{35,l}, K. Begzsuren²⁵, J. V. Bennett⁵, N. Berger²⁶, M. Bertani^{23A}, D. Bettoni^{24A}, F. Bianchi^{58A,58C}, J. Biernat⁵⁹, J. Bloms⁵², I. Boyko²⁷, R. A. Briere⁵, H. Cai⁶⁰, X. Cai^{1,43}, A. Calcaterra^{23A}, G. F. Cao^{1,47}, N. Cao^{1,47}, S. A. Cetin^{46B}, J. Chai^{58C}, J. F. Chang^{1,43}, W. L. Chang^{1,47}, G. Chelkov^{27,b,c}, D. Y. Chen⁶, G. Chen¹, H. S. Chen^{1,47}, J. C. Chen¹, M. L. Chen^{1,43}, S. J. Chen³³, Y. B. Chen^{1,43}, W. Cheng^{58C}, G. Cibinetto^{24A}, F. Cossio^{58C}, X. F. Cui³⁴, H. L. Dai^{1,43}, J. P. Dai^{38,h}, X. C. Dai^{1,47}, A. Dbeysy¹⁵, D. Dedovich²⁷, Z. Y. Deng¹, A. Denig²⁶, I. Denysenko²⁷, M. Destefanis^{58A,58C}, F. De Mori^{58A,58C}, Y. Ding³¹, C. Dong³⁴, J. Dong^{1,43}, L. Y. Dong^{1,47}, M. Y. Dong^{1,43,47}, Z. L. Dou³³, S. X. Du⁶³, J. Z. Fan⁴⁵, J. Fang^{1,43}, S. S. Fang^{1,47}, Y. Fang¹, R. Farinelli^{24A,24B}, L. Fava^{58B,58C}, F. Feldbauer⁴, G. Felici^{23A}, C. Q. Feng^{55,43}, M. Fritsch⁴, C. D. Fu¹, Y. Fu¹, Q. Gao¹, X. L. Gao^{55,43}, Y. Gao⁵⁶, Y. Gao⁴⁵, Y. G. Gao⁶, Z. Gao^{55,43}, B. Garillon²⁶, I. Garzia^{24A}, E. M. Gersabeck⁵⁰, A. Gilman⁵¹, K. Goetzen¹¹, L. Gong³⁴, W. X. Gong^{1,43}, W. Gradl²⁶, M. Greco^{58A,58C}, L. M. Gu³³, M. H. Gu^{1,43}, S. Gu², Y. T. Gu¹³, A. Q. Guo²², L. B. Guo³², R. P. Guo³⁶, Y. P. Guo²⁶, A. Guskov²⁷, S. Han⁶⁰, X. Q. Hao¹⁶, F. A. Harris⁴⁸, K. L. He^{1,47}, F. H. Heinsius⁴, T. Held⁴, Y. K. Heng^{1,43,47}, M. Himmelreich^{11,g}, Y. R. Hou⁴⁷, Z. L. Hou¹, H. M. Hu^{1,47}, J. F. Hu^{38,h}, T. Hu^{1,43,47}, Y. Hu¹, G. S. Huang^{55,43}, J. S. Huang¹⁶, X. T. Huang³⁷, X. Z. Huang³³, N. Huesken⁵², T. Hussain⁵⁷, W. Ikegami Andersson⁵⁹, W. Imoehl²², M. Irshad^{55,43}, Q. Ji¹, Q. P. Ji¹⁶, X. B. Ji^{1,47}, X. L. Ji^{1,43}, H. L. Jiang³⁷, X. S. Jiang^{1,43,47}, X. Y. Jiang³⁴, J. B. Jiao³⁷, Z. Jiao¹⁸, D. P. Jin^{1,43,47}, S. Jin³³, Y. Jin⁴⁹, T. Johansson⁵⁹, N. Kalantar-Nayestanaki²⁹, X. S. Kang³¹, R. Kappert²⁹, M. Kavatsyuk²⁹, B. C. Ke¹, I. K. Keshk⁴, A. Khoukaz⁵², P. Kiese²⁶, R. Kiuchi¹, R. Kliemt¹¹, L. Koch²⁸, O. B. Kolcu^{46B,f}, B. Kopf⁴, M. Kuemmel⁴, M. Kuessner⁴, A. Kupsc⁵⁹, M. Kurth¹, M. G. Kurth^{1,47}, W. Kühn²⁸, J. S. Lange²⁸, P. Larin¹⁵, L. Lavezzi^{58C}, H. Leithoff²⁶, T. Lenz²⁶, C. Li⁵⁹, Cheng Li^{55,43}, D. M. Li⁶³, F. Li^{1,43}, F. Y. Li^{35,l}, G. Li¹, H. B. Li^{1,47}, H. J. Li^{9,j}, J. C. Li¹, J. W. Li⁴¹, Ke Li¹, L. K. Li¹, Lei Li³, P. L. Li^{55,43}, P. R. Li³⁰, Q. Y. Li³⁷, W. D. Li^{1,47}, W. G. Li¹, X. H. Li^{55,43}, X. L. Li³⁷, X. N. Li^{1,43}, Z. B. Li⁴⁴, Z. Y. Li⁴⁴, H. Liang^{1,47}, H. Liang^{55,43}, Y. F. Liang⁴⁰, Y. T. Liang²⁸, G. R. Liao¹², L. Z. Liao^{1,47}, J. Libby²¹, C. X. Lin⁴⁴, D. X. Lin¹⁵, Y. J. Lin¹³, B. Liu^{38,h}, B. J. Liu¹, C. X. Liu¹, D. Liu^{55,43}, D. Y. Liu^{38,h}, F. H. Liu³⁹, Fang Liu¹, Feng Liu⁶, H. B. Liu¹³, H. M. Liu^{1,47}, Huanhuan Liu¹, Huihui Liu¹⁷, J. B. Liu^{55,43}, J. Y. Liu^{1,47}, K. Liu¹, K. Y. Liu³¹, Ke Liu⁶, L. Y. Liu¹³, Q. Liu⁴⁷, S. B. Liu^{55,43}, T. Liu^{1,47}, X. Liu³⁰, X. Y. Liu^{1,47}, Y. B. Liu³⁴, Z. A. Liu^{1,43,47}, Zhiqing Liu³⁷, Y. F. Long^{35,l}, X. C. Lou^{1,43,47}, H. J. Lu¹⁸, J. D. Lu^{1,47}, J. G. Lu^{1,43}, Y. Lu¹, Y. P. Lu^{1,43}, C. L. Luo³², M. X. Luo⁶², P. W. Luo⁴⁴, T. Luo^{9,j}, X. L. Luo^{1,43}, S. Lusso^{58C}, X. R. Lyu⁴⁷, F. C. Ma³¹, H. L. Ma¹, L. L. Ma³⁷, M. M. Ma^{1,47}, Q. M. Ma¹, X. N. Ma³⁴, X. X. Ma^{1,47}, X. Y. Ma^{1,43}, Y. M. Ma³⁷, F. E. Maas¹⁵, M. Maggiora^{58A,58C}, S. Maldaner²⁶, S. Malde⁵³, Q. A. Malik⁵⁷, A. Mangoni^{23B}, Y. J. Mao^{35,l}, Z. P. Mao¹, S. Marcello^{58A,58C}, Z. X. Meng⁴⁹, J. G. Messchendorp²⁹, G. Mezzadri^{24A}, J. Min^{1,43}, T. J. Min³³, R. E. Mitchell²², X. H. Mo^{1,43,47}, Y. J. Mo⁶, C. Morales Morales¹⁵, N. Yu. Muchnoi^{10,d}, H. Muramatsu⁵¹, A. Mustafa⁴, S. Nakhoul^{11,g}, Y. Nefedov²⁷, F. Nerling^{11,g}, I. B. Nikolaev^{10,d}, Z. Ning^{1,43}, S. Nisar^{8,k}, S. L. Niu^{1,43}, S. L. Olsen⁴⁷, Q. Ouyang^{1,43,47}, S. Pacetti^{23B}, Y. Pan^{55,43}, M. Papenbrock⁵⁹, P. Patteri^{23A}, M. Pelizaeus⁴, H. P. Peng^{55,43}, K. Peters^{11,g}, J. Pettersson⁵⁹, J. L. Ping³², R. G. Ping^{1,47}, A. Pitka⁴, R. Poling⁵¹, V. Prasad^{55,43}, H. R. Qi², M. Qi³³, T. Y. Qi², S. Qian^{1,43}, C. F. Qiao⁴⁷, N. Qin⁶⁰, X. P. Qin¹³, X. S. Qin⁴, Z. H. Qin^{1,43}, J. F. Qiu¹, S. Q. Qu³⁴, K. H. Rashid^{57,i}, K. Ravindran²¹, C. F. Redmer²⁶, M. Richter⁴, A. Rivetti^{58C}, V. Rodin²⁹, M. Rolo^{58C}, G. Rong^{1,47}, Ch. Rosner¹⁵, M. Rump⁵², A. Sarantsev^{27,e}, M. Savrié^{24B}, Y. Schelhaas²⁶, K. Schoenning⁵⁹, W. Shan¹⁹, X. Y. Shan^{55,43}, M. Shao^{55,43}, C. P. Shen², P. X. Shen³⁴, X. Y. Shen^{1,47}, H. Y. Sheng¹, X. Shi^{1,43}, X. D. Shi^{55,43}, J. J. Song³⁷, Q. Q. Song^{55,43}, X. Y. Song¹, S. Sosio^{58A,58C}, C. Sowa⁴, S. Spataro^{58A,58C}, F. F. Sui³⁷, G. X. Sun¹, J. F. Sun¹⁶, L. Sun⁶⁰, S. S. Sun^{1,47}, X. H. Sun¹, Y. J. Sun^{55,43}, Y. K. Sun^{55,43}, Y. Z. Sun¹, Z. J. Sun^{1,43}, Z. T. Sun¹, Y. T. Tan^{55,43}, C. J. Tang⁴⁰, G. Y. Tang¹, X. Tang¹, V. Thoren⁵⁹, B. Tsednee²⁵, I. Uman^{46D}, B. Wang¹, B. L. Wang⁴⁷, C. W. Wang³³, D. Y. Wang^{35,l}, K. Wang^{1,43}, L. L. Wang¹, L. S. Wang¹, M. Wang³⁷, M. Z. Wang^{35,l}, Meng Wang^{1,47}, P. L. Wang¹, R. M. Wang⁶¹, W. P. Wang^{55,43}, X. Wang^{35,l}, X. F. Wang³⁰, X. L. Wang^{9,j}, Y. Wang⁴⁴, Y. Wang^{55,43}, Y. F. Wang^{1,43,47}, Y. Q. Wang¹, Z. Wang^{1,43}, Z. G. Wang^{1,43}, Z. Y. Wang¹, Zongyuan Wang^{1,47}, T. Weber⁴, D. H. Wei¹², P. Weidenkaff²⁶, F. Weidner⁵², H. W. Wen³², S. P. Wen¹, U. Wiedner⁴, G. Wilkinson⁵³, M. Wolke⁵⁹, L. H. Wu¹, L. J. Wu^{1,47}, Z. Wu^{1,43}, L. Xia^{55,43}, Y. Xia²⁰, S. Y. Xiao¹, Y. J. Xiao^{1,47}, Z. J. Xiao³², Y. G. Xie^{1,43}, Y. H. Xie⁶, T. Y. Xing^{1,47}, X. A. Xiong^{1,47}, Q. L. Xiu^{1,43}, G. F. Xu¹, J. J. Xu³³, L. Xu¹, Q. J. Xu¹⁴, W. Xu^{1,47}, X. P. Xu⁴¹, F. Yan⁵⁶, L. Yan^{58A,58C}, W. B. Yan^{55,43}, W. C. Yan², Y. H. Yan²⁰, H. J. Yang^{38,h}, H. X. Yang¹, L. Yang⁶⁰, R. X. Yang^{55,43}, S. L. Yang^{1,47}, Y. H. Yang³³, Y. X. Yang¹², Yifan Yang^{1,47}, Z. Q. Yang²⁰, M. Ye^{1,43}, M. H. Ye⁷, J. H. Yin¹, Z. Y. You⁴⁴, B. X. Yu^{1,43,47}, C. X. Yu³⁴, J. S. Yu²⁰, T. Yu⁵⁶, C. Z. Yuan^{1,47}, X. Q. Yuan^{35,l}, Y. Yuan¹, A. Yuncu^{46B,a}, A. A. Zafar⁵⁷, Y. Zeng²⁰, B. X. Zhang¹, B. Y. Zhang^{1,43}, C. C. Zhang¹, D. H. Zhang¹, H. H. Zhang⁴⁴, H. Y. Zhang^{1,43}, J. Zhang^{1,47}, J. L. Zhang⁶¹,

J. Q. Zhang⁴, J. W. Zhang^{1,43,47}, J. Y. Zhang¹, J. Z. Zhang^{1,47}, K. Zhang^{1,47}, L. Zhang¹, S. F. Zhang³³, T. J. Zhang^{38,h}, X. Y. Zhang³⁷, Y. Zhang^{55,43}, Y. H. Zhang^{1,43}, Y. T. Zhang^{55,43}, Yang Zhang¹, Yao Zhang¹, Yi Zhang^{9,j}, Yu Zhang⁴⁷, Z. H. Zhang⁶, Z. P. Zhang⁵⁵, Z. Y. Zhang⁶⁰, G. Zhao¹, J. W. Zhao^{1,43}, J. Y. Zhao^{1,47}, J. Z. Zhao^{1,43}, Lei Zhao^{55,43}, Ling Zhao¹, M. G. Zhao³⁴, Q. Zhao¹, S. J. Zhao⁶³, T. C. Zhao¹, Y. B. Zhao^{1,43}, Z. G. Zhao^{55,43}, A. Zhemchugov^{27,b}, B. Zheng⁵⁶, J. P. Zheng^{1,43}, Y. Zheng^{35,l}, Y. H. Zheng⁴⁷, B. Zhong³², L. Zhou^{1,43}, L. P. Zhou^{1,47}, Q. Zhou^{1,47}, X. Zhou⁶⁰, X. K. Zhou⁴⁷, X. R. Zhou^{55,43}, Xiaoyu Zhou²⁰, Xu Zhou²⁰, A. N. Zhu^{1,47}, J. Zhu³⁴, J. Zhu⁴⁴, K. Zhu¹, K. J. Zhu^{1,43,47}, S. H. Zhu⁵⁴, W. J. Zhu³⁴, X. L. Zhu⁴⁵, Y. C. Zhu^{55,43}, Y. S. Zhu^{1,47}, Z. A. Zhu^{1,47}, J. Zhuang^{1,43}, B. S. Zou¹, J. H. Zou¹

(BESIII Collaboration)

- ¹ *Institute of High Energy Physics, Beijing 100049, People's Republic of China*
² *Beihang University, Beijing 100191, People's Republic of China*
³ *Beijing Institute of Petrochemical Technology, Beijing 102617, People's Republic of China*
⁴ *Bochum Ruhr-University, D-44780 Bochum, Germany*
⁵ *Carnegie Mellon University, Pittsburgh, Pennsylvania 15213, USA*
⁶ *Central China Normal University, Wuhan 430079, People's Republic of China*
⁷ *China Center of Advanced Science and Technology, Beijing 100190, People's Republic of China*
⁸ *COMSATS University Islamabad, Lahore Campus, Defence Road, Off Raiwind Road, 54000 Lahore, Pakistan*
⁹ *Fudan University, Shanghai 200443, People's Republic of China*
¹⁰ *G.I. Budker Institute of Nuclear Physics SB RAS (BINP), Novosibirsk 630090, Russia*
¹¹ *GSI Helmholtzcentre for Heavy Ion Research GmbH, D-64291 Darmstadt, Germany*
¹² *Guangxi Normal University, Guilin 541004, People's Republic of China*
¹³ *Guangxi University, Nanning 530004, People's Republic of China*
¹⁴ *Hangzhou Normal University, Hangzhou 310036, People's Republic of China*
¹⁵ *Helmholtz Institute Mainz, Johann-Joachim-Becher-Weg 45, D-55099 Mainz, Germany*
¹⁶ *Henan Normal University, Xinxiang 453007, People's Republic of China*
¹⁷ *Henan University of Science and Technology, Luoyang 471003, People's Republic of China*
¹⁸ *Huangshan College, Huangshan 245000, People's Republic of China*
¹⁹ *Hunan Normal University, Changsha 410081, People's Republic of China*
²⁰ *Hunan University, Changsha 410082, People's Republic of China*
²¹ *Indian Institute of Technology Madras, Chennai 600036, India*
²² *Indiana University, Bloomington, Indiana 47405, USA*
²³ *(A)INFN Laboratori Nazionali di Frascati, I-00044, Frascati, Italy; (B)INFN and University of Perugia, I-06100, Perugia, Italy*
²⁴ *(A)INFN Sezione di Ferrara, I-44122, Ferrara, Italy; (B)University of Ferrara, I-44122, Ferrara, Italy*
²⁵ *Institute of Physics and Technology, Peace Ave. 54B, Ulaanbaatar 13330, Mongolia*
²⁶ *Johannes Gutenberg University of Mainz, Johann-Joachim-Becher-Weg 45, D-55099 Mainz, Germany*
²⁷ *Joint Institute for Nuclear Research, 141980 Dubna, Moscow region, Russia*
²⁸ *Justus-Liebig-Universitaet Giessen, II. Physikalisches Institut, Heinrich-Buff-Ring 16, D-35392 Giessen, Germany*
²⁹ *KVI-CART, University of Groningen, NL-9747 AA Groningen, The Netherlands*
³⁰ *Lanzhou University, Lanzhou 730000, People's Republic of China*
³¹ *Liaoning University, Shenyang 110036, People's Republic of China*
³² *Nanjing Normal University, Nanjing 210023, People's Republic of China*
³³ *Nanjing University, Nanjing 210093, People's Republic of China*
³⁴ *Nankai University, Tianjin 300071, People's Republic of China*
³⁵ *Peking University, Beijing 100871, People's Republic of China*
³⁶ *Shandong Normal University, Jinan 250014, People's Republic of China*
³⁷ *Shandong University, Jinan 250100, People's Republic of China*
³⁸ *Shanghai Jiao Tong University, Shanghai 200240, People's Republic of China*
³⁹ *Shanxi University, Taiyuan 030006, People's Republic of China*
⁴⁰ *Sichuan University, Chengdu 610064, People's Republic of China*
⁴¹ *Soochow University, Suzhou 215006, People's Republic of China*
⁴² *Southeast University, Nanjing 211100, People's Republic of China*

⁴³ *State Key Laboratory of Particle Detection and Electronics, Beijing 100049, Hefei 230026, People's Republic of China*

⁴⁴ *Sun Yat-Sen University, Guangzhou 510275, People's Republic of China*

⁴⁵ *Tsinghua University, Beijing 100084, People's Republic of China*

⁴⁶ (A)*Ankara University, 06100 Tandogan, Ankara, Turkey;* (B)*Istanbul Bilgi University, 34060 Eyup, Istanbul, Turkey;*
(C)*Uludag University, 16059 Bursa, Turkey;* (D)*Near East University, Nicosia, North Cyprus, Mersin 10, Turkey*

⁴⁷ *University of Chinese Academy of Sciences, Beijing 100049, People's Republic of China*

⁴⁸ *University of Hawaii, Honolulu, Hawaii 96822, USA*

⁴⁹ *University of Jinan, Jinan 250022, People's Republic of China*

⁵⁰ *University of Manchester, Oxford Road, Manchester, M13 9PL, United Kingdom*

⁵¹ *University of Minnesota, Minneapolis, Minnesota 55455, USA*

⁵² *University of Muenster, Wilhelm-Klemm-Str. 9, 48149 Muenster, Germany*

⁵³ *University of Oxford, Keble Rd, Oxford, UK OX13RH*

⁵⁴ *University of Science and Technology Liaoning, Anshan 114051, People's Republic of China*

⁵⁵ *University of Science and Technology of China, Hefei 230026, People's Republic of China*

⁵⁶ *University of South China, Hengyang 421001, People's Republic of China*

⁵⁷ *University of the Punjab, Lahore-54590, Pakistan*

⁵⁸ (A)*University of Turin, I-10125, Turin, Italy;* (B)*University of Eastern Piedmont, I-15121, Alessandria, Italy;* (C)*INFN, I-10125, Turin, Italy*

⁵⁹ *Uppsala University, Box 516, SE-75120 Uppsala, Sweden*

⁶⁰ *Wuhan University, Wuhan 430072, People's Republic of China*

⁶¹ *Xinyang Normal University, Xinyang 464000, People's Republic of China*

⁶² *Zhejiang University, Hangzhou 310027, People's Republic of China*

⁶³ *Zhengzhou University, Zhengzhou 450001, People's Republic of China*

^a *Also at Bogazici University, 34342 Istanbul, Turkey*

^b *Also at the Moscow Institute of Physics and Technology, Moscow 141700, Russia*

^c *Also at the Functional Electronics Laboratory, Tomsk State University, Tomsk, 634050, Russia*

^d *Also at the Novosibirsk State University, Novosibirsk, 630090, Russia*

^e *Also at the NRC "Kurchatov Institute", PNPI, 188300, Gatchina, Russia*

^f *Also at Istanbul Arel University, 34295 Istanbul, Turkey*

^g *Also at Goethe University Frankfurt, 60323 Frankfurt am Main, Germany*

^h *Also at Key Laboratory for Particle Physics, Astrophysics and Cosmology, Ministry of Education; Shanghai Key Laboratory for Particle Physics and Cosmology; Institute of Nuclear and Particle Physics, Shanghai 200240, People's Republic of China*

ⁱ *Also at Government College Women University, Sialkot - 51310. Punjab, Pakistan.*

^j *Also at Key Laboratory of Nuclear Physics and Ion-beam Application (MOE) and Institute of Modern Physics, Fudan University, Shanghai 200443, People's Republic of China*

^k *Also at Harvard University, Department of Physics, Cambridge, MA, 02138, USA*

^l *Also at State Key Laboratory of Nuclear Physics and Technology, Peking University, Beijing 100871, People's Republic of China*

(Dated: October 14, 2019)

Using a total of 11.0 fb^{-1} of e^+e^- collision data with center-of-mass energies between 4.009 GeV and 4.6 GeV and collected with the BESIII detector at BEPCII, we measure fifteen exclusive cross sections and effective form factors for the process $e^+e^- \rightarrow \Xi^-\Xi^+$ by means of a single baryon-tag method. After performing a fit to the dressed cross section of $e^+e^- \rightarrow \Xi^-\Xi^+$, no significant $\psi(4230)$ or $\psi(4260)$ resonance is observed in the $\Xi^-\Xi^+$ final states, and upper limits at the 90% confidence level on $\Gamma_{ee}\mathcal{B}$ for the processes $\psi(4230)/\psi(4260) \rightarrow \Xi^-\Xi^+$ are determined. In addition, an excited Ξ baryon at $1820 \text{ MeV}/c^2$ is observed with a statistical significance of 5.1σ , and the mass and width are measured to be $M = (1825.5 \pm 4.7 \pm 4.7) \text{ MeV}/c^2$ and $\Gamma = (17.0 \pm 15.0 \pm 7.9) \text{ MeV}$, which confirms the existence of the $J^P = \frac{3}{2}^-$ state $\Xi(1820)$.

PACS numbers: 13.20.Gd, 13.30.-a, 14.20.Pt

¹ In the last decade, a series of charmonium-like states have ³ been observed at e^+e^- colliders. The study of the pro- ⁴ duction of charmonium-like states with the quantum number $J^{PC} = 1^{--}$ above open charm threshold in e^+e^- annihi-

lations and their subsequent two-body hadronic decays provides a test for QCD calculations [1, 2]. According to potential models, there are five vector charmonium states between the $1D$ state ($\psi(3773)$) and $4.7 \text{ GeV}/c^2$, namely, the $3S$, $2D$, $4S$, $3D$, and $5S$ states [1]. From experimental studies, besides the three well-established structures observed in the inclusive hadronic cross section [3], *i.e.*, $\psi(4040)$, $\psi(4160)$, and $\psi(4415)$, five new states, *i.e.*, $\psi(4230)$, $\psi(4260)$, $\psi(4360)$, $\psi(4634)$ and $\psi(4660)$ have been reported in initial state radiation (ISR) processes, *i.e.*, $e^+e^- \rightarrow \gamma_{ISR}\pi^+\pi^-J/\psi$ or $e^+e^- \rightarrow \gamma_{ISR}\pi^+\pi^-\psi(3686)$ at the B factories [4] or in direct production processes at the CLEO [5] and BESIII experiments [6]. Surprisingly, up to now, no evidence for baryon anti-baryon pairs above open charm production associated with these states has been found except for the $\psi(4634)$ resonance observed in $\Lambda_c^+\bar{\Lambda}_c^-$ [7]. Although the BESIII Collaboration previously performed a search for baryonic decays of $\psi(4040)$ [8], including $\Xi^-\bar{\Xi}^+$ final states based on a full reconstruction method, no candidates were observed. The overpopulation of structures in this mass region and the mismatch of the properties between the potential model predictions and experimental measurements make them good candidates for exotic states. Various scenarios, which interpret one or some of them as hybrid states, tetraquark states, or molecular states [9], have been proposed.

The electromagnetic structure of hadrons, parameterized in terms of electromagnetic form factors (EMFFs) [10], provides a key to understanding QCD effects in bound states. While the nucleon has been studied rigorously for more than sixty years, new techniques and the availability of data with larger statistics from modern facilities have given rise to a renewed interest in the field, *i.e.*, the proton radius puzzle [11]. The access to hyperon structure by EMFFs provides an extra dimension that inspires measurements of exclusive cross sections and EMFFs for baryon anti-baryon pairs above open charm threshold.

The constituent quark model has been very successful in describing the ground state of the flavor SU(3) octet and decuplet baryons [3, 12]. However, some observed excited states do not agree well with the theoretical prediction. It is thus important to study such unusual states, both to probe the limitation of the quark models and to spot unrevealed aspects of the QCD description of the structure of hadron resonances. Intriguingly, the Ξ resonances with strangeness $S = -2$ may provide important information on the latter aspect. Although, there has been significant progress in the experimental studies of charmed baryons by the BaBar [13], LHCb [14], and Belle [15, 16] collaborations, doubly-charm baryons by the LHCb collaboration [17], doubly-strange baryons by the Belle collaboration [18, 19], the studies of excited Ξ states are still sparse [3]. Neither the first radial excitation with spin-parity of $J^P = \frac{1}{2}^+$ nor a first orbital excitation with $J^P = \frac{1}{2}^-$ have been identified. Determination of the resonance parameters of the first excited state is a vital test of our understanding of the structure of Ξ resonances, where one of candidates for

the first excited state is $\Xi(1690)$ with a three-star rating on a four-star scale [3], the second one is $\Xi(1620)$ with one-star rating, and another excited state is $\Xi(1820)$ with a three-star rating [3], for which the spin was previously determined to be $J = \frac{3}{2}$ [20], and subsequently the parity was determined to be negative and the spin confirmed to be $J^P = \frac{3}{2}^-$ by another experiment [21].

In this Letter, we present a measurement of the Born cross section and the effective form factors (EFF) [10] for the process $e^+e^- \rightarrow \Xi^-\bar{\Xi}^+$, an estimation of the upper limit on $\Gamma_{ee}\mathcal{B}(\psi(4230)/\psi(4260) \rightarrow \Xi^-\bar{\Xi}^+)$ at the 90% confidence level (CL), and the observation of an excited Ξ baryon at 1820 MeV/ c^2 . The dataset used in this analysis corresponds to a total of 11.0 fb^{-1} of e^+e^- collision data [10] collected at center-of-mass (CM) energies from 4.009 GeV to 4.6 GeV with the BESIII detector [22] at BEPCII [23].

The selection of $e^+e^- \rightarrow \Xi^-\bar{\Xi}^+$ events with a full reconstruction method has low-reconstruction efficiency. Here, to achieve higher efficiency, a single baryon Ξ^- tag technique is employed, *i.e.*, only one Ξ^- baryon is reconstructed by the $\pi^-\Lambda$ decay mode with $\Lambda \rightarrow p\pi^-$, and the anti-baryon $\bar{\Xi}^+$ is extracted from the recoil side (unless otherwise noted, the charge-conjugate state of the Ξ^- mode is included by default below). To determine the detection efficiency for the decay $e^+e^- \rightarrow \Xi^-\bar{\Xi}^+$, 100,000 simulated events are generated for each energy point according to phase space using the KKMC generator [24], which includes the ISR effect. The Ξ^- is simulated in its decay to the $\pi^-\Lambda$ mode with the subsequent decay $\Lambda \rightarrow p\pi^-$ via EVTGEN [25], and the anti-baryons are allowed to decay inclusively. The response of the BESIII detector is modeled with Monte Carlo (MC) simulations using a framework based on GEANT4 [26]. Large simulated samples of generic $e^+e^- \rightarrow$ hadrons events (‘inclusive MC’) are used to estimate background conditions.

Charged tracks are required to be reconstructed in the main drift chamber (MDC) with good helical fits and within the angular coverage of the MDC ($|\cos\theta| < 0.93$, where θ is the polar angle with respect to the e^+ beam direction). Information from the specific energy deposition (dE/dx) measured in the MDC combined with the time-of-flight (TOF) is used to form particle identification (PID) confidence levels for the hypotheses of a pion, kaon, and proton. Each track is assigned to the particle type with the highest CL. Events with at least two negatively charged pions and one proton are kept for further analysis.

To reconstruct Λ candidates, a secondary vertex fit is applied to all $p\pi^-$ combinations; the ones characterized by $\chi^2 < 500$ are kept for further analysis. The $p\pi^-$ invariant mass is required to be within 5 MeV/ c^2 of the nominal Λ mass, determined by optimizing the figure of merit $\frac{S}{\sqrt{S+B}}$ based on the MC simulation, where S is the number of signal MC events and B is the number of the background events expected from simulation. To further suppress background from non- Λ events, the Λ decay length is required to be greater than

114 zero, where negative decay lengths are caused by the limited
115 detector resolution.

116 The Ξ^- candidates are reconstructed with a similar strategy
117 using a secondary vertex fit, and the candidate with the minimum
118 value of $|M_{\pi^- \Lambda} - m_{\Xi^-}|$ from all $\pi^- \Lambda$ combinations
119 is selected, where $M_{\pi^- \Lambda}$ is the invariant mass of the $\pi^- \Lambda$
120 pair, and m_{Ξ^-} is the nominal mass of Ξ^- from the PDG [3].
121 Further $M_{\pi^- \Lambda}$ is required to be within 10 MeV/ c^2 of the nominal
122 Ξ^- mass, and the Ξ^- decay length L_{Ξ^-} is required to be
123 greater than 0.

124 To obtain the anti-baryon candidates Ξ^+ , we use the distribution
125 of mass recoiling against the selected $\pi^- \Lambda$ system,

$$M_{\pi^- \Lambda}^{\text{recoil}} = \sqrt{(\sqrt{s} - E_{\pi^- \Lambda})^2 - |\vec{p}_{\pi^- \Lambda}|^2}, \quad (1)$$

126 where $E_{\pi^- \Lambda}$ and $\vec{p}_{\pi^- \Lambda}$ are the energy and momentum of the
127 selected $\pi^- \Lambda$ candidate in the CM system, and \sqrt{s} is the
128 CM energy. Figure 1 shows the distribution of $M_{\pi^- \Lambda}$ versus
129 $M_{\pi^- \Lambda}^{\text{recoil}}$ for all 15 considered energy points.

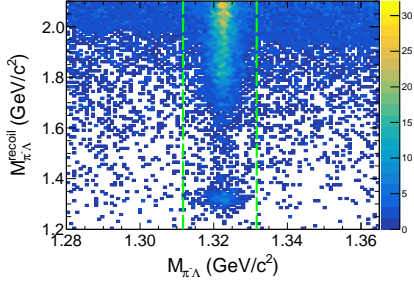


FIG. 1. Distribution of $M_{\pi^- \Lambda}$ versus $M_{\pi^- \Lambda}^{\text{recoil}}$ for sum of 15 energy
150 points. The dashed lines denote the Ξ^- signal region.

130 The signal yields for the decay $e^+e^- \rightarrow \Xi^- \Xi^+$ at each
131 energy point are determined by performing an extended maximum
132 likelihood fit to the $M_{\pi^- \Lambda}^{\text{recoil}}$ spectrum in the range from
133 1.2 GeV/ c^2 to 1.5 GeV/ c^2 . In the fit, the signal shape for the
134 decay $e^+e^- \rightarrow \Xi^- \Xi^+$ at each energy point is represented by
135 the simulated MC shape. After applying the same event selection
136 as the data on the inclusive MC samples at each CM
137 energy, it is found that few background events remain at each
138 energy point coming from $e^+e^- \rightarrow \pi^+ \pi^- J/\psi$, $J/\psi \rightarrow \Lambda \bar{\Lambda}$
139 events, and they are distributed smoothly in the region of interest
140 and can be described by a second-order polynomial function.
141 Figure 2 shows the $M_{\pi^- \Lambda}^{\text{recoil}}$ distributions for the decay
142 $e^+e^- \rightarrow \Xi^- \Xi^+$ at each energy point.

144 The Born cross section for $e^+e^- \rightarrow \Xi^- \Xi^+$ is calculated by

$$\sigma^B(s) = \frac{N_{\text{obs}}}{2\mathcal{L}(1 + \delta)|1 + \Pi|\epsilon\mathcal{B}(\Xi^- \rightarrow \pi^- \Lambda)\mathcal{B}(\Lambda \rightarrow p\pi^-)}, \quad (2)$$

145 where N_{obs} is the number of the observed signal events, \mathcal{L} is
146 the integrated luminosity related to the CM energy, $(1 + \delta)$
147 is the ISR correction factor, $|1 + \Pi|$ is the vacuum polarization
148 correction factor, ϵ is the detection efficiency, and

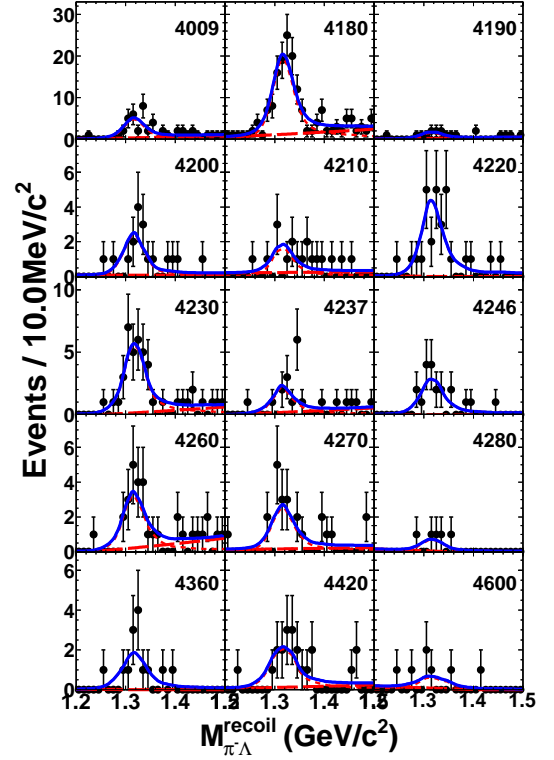


FIG. 2. Fit to the recoil mass spectra of $\pi^- \Lambda$ at each energy point in
units of MeV/ c^2 . Dots with error bars are data, the blue solid lines
show the fit result, the red short-dashed lines are for signal, and the
red long-dashed ones are for the smooth background.

149 $\mathcal{B}(\Xi \rightarrow \pi^- \Lambda)$ and $\mathcal{B}(\Lambda \rightarrow p\pi^-)$ are the branching fractions
150 taken from the PDG [3]. The ISR correction factor is obtained
151 using the QED calculation as described in Ref. [27] and taking
152 the formula used to fit the cross section measured in this analysis
153 parameterized after two iterations as input. The measured cross
154 sections and EFFs are shown in Fig. 3 and summarized in the
155 Supplemental Material [10]. The Supplemental Material also contains
156 the details of the cross section and EFF calculations.

A maximum likelihood method is used to fit the dressed
cross section $\sigma^{\text{dressed}} = \sigma^B|1 + \Pi|$ for the process $e^+e^- \rightarrow$
 $\Xi^- \Xi^+$ parameterized as the coherent sum of a power-law
function plus a Breit-Wigner (BW) function for $\psi(4230)$ or
 $\psi(4260)$,

$$\sigma^{\text{dressed}}(\sqrt{s}) = |c_0 \frac{\sqrt{P(\sqrt{s})}}{s^n} + e^{i\phi} \text{BW}(\sqrt{s}) \sqrt{\frac{P(\sqrt{s})}{P(M)}}|^2, \quad (3)$$

where the mass, M , and total width, Γ , are fixed to the
 $\psi(4230)/\psi(4260)$ resonance with PDG values [3], ϕ is the
relative phase between the BW function,

$$\text{BW}(\sqrt{s}) = \frac{\sqrt{12\pi\Gamma_{ee}\mathcal{B}}}{s - M^2 + iM\Gamma}, \quad (4)$$

and power function, n is a free fit parameter, and $P(\sqrt{s})$ is the

two-body phase space factor. The $\psi(4230)$ and $\psi(4260) \rightarrow \Xi^- \bar{\Xi}^+$ processes are found to be not significant. Therefore, upper limits on the products of the two-electron partial width and the branching fractions of $\psi(4230)$ and $\psi(4260) \rightarrow \Xi^- \bar{\Xi}^+$ ($\Gamma_{ee} \mathcal{B}$) at the 90% confidence level are estimated using a Bayesian approach [28] to be $\Gamma_{ee} \mathcal{B}_{\psi(4230)} < 0.33 \times 10^{-3}$ eV and $\Gamma_{ee} \mathcal{B}_{\psi(4260)} < 0.27 \times 10^{-3}$ eV taking into account the systematic uncertainty described later. Here the masses and widths of $\psi(4230)$ and $\psi(4260)$ are changed by all combinations of $\pm 1\sigma$, and the estimation of the upper limits repeated. The largest ones are taken as the final results. Figure 3 shows the fit to the dressed cross section assuming the $\psi(4230)$ or the $\psi(4260)$ resonance. Including systematic uncertainties, the significance for both resonances is calculated to be about 2.0σ .

The EFF for $e^+e^- \rightarrow \Xi^- \bar{\Xi}^+$ is calculated by the formula [10],

$$|G_{\text{eff}}(s)| = \sqrt{\frac{3s\sigma^B}{4\pi\alpha^2 C \beta (1 + \frac{2m_{\Xi^-}^2}{s})}}, \quad (5)$$

where α is the fine structure constant, m_{Ξ^-} is the mass of Ξ^- , the variable $\beta = \sqrt{1 - \frac{1}{\tau}}$ is the velocity, $\tau = \frac{s}{4m_{\Xi^-}^2}$, and the Coulomb correction factor C [29, 30] parameterizes the electro-magnetic interaction between the outgoing baryon and anti-baryon. For neutral baryons, the Coulomb factor is unity, while for point-like charged fermions $C = \frac{\pi\alpha}{\beta} \cdot \frac{\sqrt{1-\beta^2}}{1-e^{-\frac{\pi\alpha}{\beta}}}$ [31–33]. Figure 3 shows the measured EFFs of $e^+e^- \rightarrow \Xi^- \bar{\Xi}^+$.

Based on the selected data for the sum of 15 energy points, an excited Ξ baryon is observed in the $M_{\pi^- \Lambda}^{\text{recoil}}$ range from 1.6 GeV/ c^2 to 2.1 GeV/ c^2 . Figure 4 shows a fit to the recoil mass spectrum of $\pi^- \Lambda$, where the signal is described by a BW function convolved with a double Gaussian function, and the background is described by a 2^{nd} order Chebyshev polynomial, where the resolution width of Gaussian function is fixed according to the MC simulation. The number of signal events is 288 ± 66 , and the mass and width are measured to be $M = (1825.5 \pm 4.7)$ MeV/ c^2 and $\Gamma = (17.0 \pm 15.0)$ MeV, where the uncertainties are statistical only. The statistical significance of the 1820 MeV resonance is estimated to be 5.1 standard deviations.

Systematic uncertainties on the measurements of the cross section originate from the luminosity measurement, branching fractions of $\Xi^- \rightarrow \pi^- \Lambda$ and $\Lambda \rightarrow p\pi^-$, detection efficiency, ISR correction factor, line-shape structure, angular distribution, and the fit procedure. The uncertainty due to the vacuum polarization is negligible. The integrated luminosity is measured with a precision of 1.0% [34]. The branching fraction uncertainties for $\Xi^- \rightarrow \pi^- \Lambda$ and $\Lambda \rightarrow p\pi^-$ are 0.1% and 0.8% from the PDG [3]. The systematic sources of the uncertainty for the detection efficiency include the Ξ^- reconstruction, the mass windows of Ξ^-/Λ , and the decay lengths of Ξ^-/Λ . The Ξ^- reconstruction is studied using the

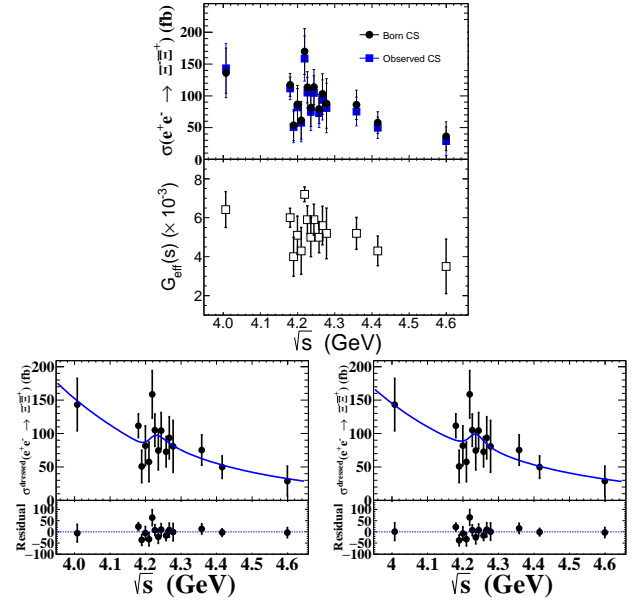


FIG. 3. Top: cross section (points with error bars) and EFF (open boxes with error bars). Bottom: fits to the dressed cross sections at CM energies from 4.009 to 4.6 GeV with the assumptions of a power-law function plus a $\psi(4230)$ resonance function (Left) and a $\psi(4260)$ resonance function (Right), where the dots with error bars are the dressed cross sections and the solid lines show the fit results.

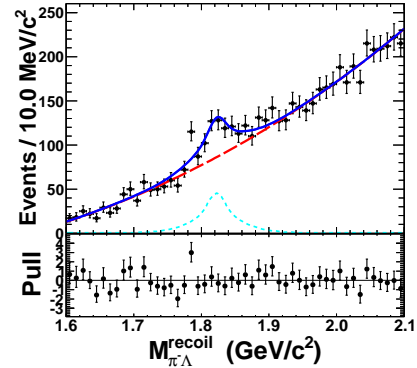


FIG. 4. Fit to the recoil mass of $\pi\Lambda$ of the combined data of the 15 energy points in the range from 1.6 to 2.1 GeV/ c^2 . Dots with error bars are data, the blue solid line shows the fit result, the short-dashed line is for signal, and the long-dashed one is for the background.

same method as described in Ref. [35], and an uncertainty of 6.6% is found. The mass windows of Ξ^- and Λ are studied by varying the nominal requirements by 5.0 MeV/ c^2 , which yield uncertainties of 0.7% and 3.2%, respectively. The decay lengths of Λ and Ξ^- are studied with and without the nominal requirements, and the uncertainties are estimated to be 1.5% and 1.7%, respectively. For the ISR correction factor, we iterate the cross section measurement until $(1 + \delta)\epsilon$ converges as described in Ref. [36]. The change due to the different criteria for convergence is taken as the systematic uncertainty. The uncertainty due to the line-shape structure is estimated to be

4.8% with the assumption of $\psi(4230)/\psi(4260) \rightarrow \Xi^- \bar{\Xi}^+$. The uncertainty due to the angular distribution is estimated to be 4.0% by weighting the $\cos \theta_{\Xi}$ difference for each bin between the data and the phase space MC model, where θ_{Ξ} is the angle between Ξ and the beam directions in the e^+e^- CM system [35]. The systematic sources of the uncertainty in the fit of the $M_{\pi^-\Lambda}^{\text{recoil}}$ spectrum include the fitting range, the polynomial shape, the mass resolution, the signal shape mass windows of Ξ^-/Λ , and the decay lengths of Ξ^-/Λ . The uncertainty due to the fit range is estimated to be 3.3% by varying the mass range by $\pm 50 \text{ MeV}/c^2$. The uncertainty due to the polynomial function is estimated to be 3.3% by alternative fits with a third- or a first-order polynomial function. The mass resolution is studied by varying the nominal signal shape convolved with a Gaussian function, and the yield difference is taken as a systematic uncertainty, which is 4.0%. The effect due to the signal shape is studied by varying the resolution in the convolution of the Breit-Wigner with a Gaussian function. This gives an uncertainty of 3.2%. The effect of the MC statistics on the used signal shape is studied by using an MC sample with only 10% of the events compared to the nominal fit, and the uncertainty is 0.5%. Assuming all sources to be independent, the total systematic uncertainty on the cross section measurement for $e^+e^- \rightarrow \Xi^- \bar{\Xi}^+$ is determined to be 12.7% by the quadratic sum of these sources.

Systematic uncertainties on the measurements of the mass and width for the excited Ξ state mainly originate from the fit range, the background shape, the mass resolution and the signal shape. The fit range, the background, and signal shapes are studied with the same method as above with mass uncertainties of $1.5 \text{ MeV}/c^2$, $1.3 \text{ MeV}/c^2$, and $1.9 \text{ MeV}/c^2$, and width uncertainties of 5.6 MeV , 3.4 MeV and 4.5 MeV , respectively. The mass uncertainty due to the mass resolution is determined to be $3.8 \text{ MeV}/c^2$ by calibrating the resolution difference in the Ξ^- mass region with the full data sample. The total systematic uncertainties of mass and width are calculated to be $4.7 \text{ MeV}/c^2$ and 7.9 MeV , respectively, by summing independent systematic sources in quadrature.

In summary, using a total of 11.0 fb^{-1} of e^+e^- collision data above the open-charm threshold collected with the BESIII detector at the BEPCII collider, we have studied the process $e^+e^- \rightarrow \Xi^- \bar{\Xi}^+$ based on a single baryon tag technique. We have measured fifteen exclusive Born cross sections and EFFs in the range from 4.009 to $4.6 \text{ GeV}/c^2$, where the form factors for the process $e^+e^- \rightarrow \Xi^- \bar{\Xi}^+$ have not been previously measured due to limited statistics. A fit to the dressed cross section for $e^+e^- \rightarrow \Xi^- \bar{\Xi}^+$ with the assumptions of a power law dependence for continuum plus a $\psi(4230)$ or $\psi(4260)$ resonance is performed, and no significant signal for the processes $\psi(4230)$ or $\psi(4260) \rightarrow \Xi^- \bar{\Xi}^+$ is observed. The upper limits on the products of the electronic partial width and the branching fractions of $\psi(4230)$ and $\psi(4260) \rightarrow \Xi^- \bar{\Xi}^+$ are measured to be $\Gamma_{ee} \mathcal{B}_{\psi(4230)} < 0.33 \times 10^{-3} \text{ eV}$ and $\Gamma_{ee} \mathcal{B}_{\psi(4260)} < 0.27 \times 10^{-3} \text{ eV}$ at 90% CL, which may help to understand the nature of $Y(4260)$ [37, 38]. In par-

particular, charmless decays of the $Y(4260)$ are expected by the hybrid model [38]. In addition, an excited Ξ baryon at $\sim 1820 \text{ MeV}/c^2$ is observed with a statistical significance of 5.1σ , and the mass and width are measured to be $M = (1825.5 \pm 4.7 \pm 4.7) \text{ MeV}/c^2$ and $\Gamma = (17.0 \pm 15.0 \pm 7.9) \text{ MeV}$, which are consistent with the mass and width of $\Xi(1820)^-$ obtained from the PDG [3] within 1σ uncertainty. The results shed light on the structure of hyperon resonances with strangeness $S = -2$.

ACKNOWLEDGEMENT

The BESIII collaboration thanks the staff of BEPCII and the IHEP computing center for their strong support. This work is supported in part by National Key Basic Research Program of China under Contract No. 2015CB856700; China Postdoctoral Science Foundation under Contract No. 2018M630206; National Natural Science Foundation of China (NSFC) under Contracts Nos. 11521505, 11625523, 11635010, 11675184, 11705209, 11735014, 11822506, 11835012, 11875115, 11905236; Chinese Academy of Science Focused Science Grant; National 1000 Talents Program of China; the Chinese Academy of Sciences (CAS) Large-Scale Scientific Facility Program; Joint Large-Scale Scientific Facility Funds of the NSFC and CAS under Contracts Nos. U1532257, U1532258, U1732263, U1832207; CAS Key Research Program of Frontier Sciences under Contracts Nos. QYZDJ-SSW-SLH003, QYZDJ-SSW-SLH040; 100 Talents Program of CAS; INPAC and Shanghai Key Laboratory for Particle Physics and Cosmology; ERC under Contract No. 758462; German Research Foundation DFG under Contracts Nos. Collaborative Research Center CRC 1044, FOR 2359; Istituto Nazionale di Fisica Nucleare, Italy; Koninklijke Nederlandse Akademie van Wetenschappen (KNAW) under Contract No. 530-4CDP03; Ministry of Development of Turkey under Contract No. DPT2006K-120470; National Science and Technology fund; STFC (United Kingdom); The Knut and Alice Wallenberg Foundation (Sweden) under Contract No. 2016.0157; The Royal Society, UK under Contracts Nos. DH140054, DH160214; The Swedish Research Council; U. S. Department of Energy under Contracts Nos. DE-FG02-05ER41374, DE-SC-0010118, DE-SC-0012069; University of Groningen (RuG) and the Helmholtzzentrum fuer Schwerionenforschung GmbH (GSI), Darmstadt

-
- [1] N. Brambilla *et al.*, *Eur. Phys. J. C* **71**, 1534 (2011).
 - [2] R. A. Briceno *et al.*, *Chin. Phys. C* **40**, 042001 (2016).
 - [3] M. Tanabashi *et al.* (Particle Data Group), *Phys. Rev. D* **98**, 030001 (2018).
 - [4] B. Aubert *et al.* (BABAR Collaboration), *Phys. Rev. Lett.* **95**, 142001 (2005); C. Z. Yuan *et al.* (Belle Collaboration), *Phys. Rev. Lett.* **99**, 182004 (2007); B. Aubert *et al.* (BABAR Col-

- laboration), Phys. Rev. Lett. **98**, 212001 (2007); X. L. Wang *et al.* (Belle Collaboration), Phys. Rev. Lett. **99**, 142002 (2007); G. Pakhlova *et al.* (Belle Collaboration), Phys. Rev. Lett. **101**, 172001 (2008); J. P. Lees *et al.* (BABAR Collaboration), Phys. Rev. D **89**, 111103 (2014); X. L. Wang *et al.* (Belle Collaboration), Phys. Rev. D **91**, 112007 (2015); J. P. Lees *et al.* (BABAR Collaboration), Phys. Rev. D **86**, 051102(R) (2012); Z. Q. Liu *et al.* (Belle Collaboration), Phys. Rev. Lett. **110**, 252002 (2013).
- [5] T. E. Coan *et al.* (CLEO Collaboration), Phys. Rev. Lett. **96**, 162003 (2006).
- [6] M. Ablikim *et al.* (BESIII Collaboration), Phys. Rev. Lett. **114**, 092003 (2015).
- [7] G. Pakhlova *et al.* (Belle Collaboration), Phys. Rev. Lett. **101**, 172001 (2008).
- [8] M. Ablikim *et al.* (BESIII Collaboration), Phys. Rev. D **87**, no. 11, 112011 (2013).
- [9] H. X. Chen, W. Chen, X. Liu, and S. L. Zhu, Phys. Rep. **639**, (2016).
- [10] See Supplemental Material at <http://XXX> add later for a summary of number of signal events, luminosity, detection efficiency, ISR factor, vacuum polarization factor, the Born cross section, the effective form factor, statistical significance at each energy point.
- [11] R. Pohl *et al.*, Nature (London) **466**, 213 (2010).
- [12] K. T. Chao, N. Isgur and G. Karl, Phys. Rev. D **23**, 155 (1981); S. Capstick and N. Isgur, Phys. Rev. D **34**, 2809 (1986).
- [13] B. Aubert *et al.* (BaBar Collaboration), Phys. Rev. Lett. **98**, 012001 (2007).
- [14] R. Aaij *et al.* (LHCb Collaboration), Phys. Rev. Lett. **118**, no. 18, 182001 (2017).
- [15] J. Yelton *et al.* (Belle Collaboration), Phys. Rev. D **97**, no. 5, 051102 (2018).
- [16] Y. B. Li *et al.* (Belle Collaboration), Eur. Phys. J. C **78**, 928 (2018).
- [17] R. Aaij *et al.* (LHCb Collaboration), Phys. Rev. Lett. **119**, no. 11, 112001 (2017); R. Aaij *et al.* (LHCb Collaboration), Phys. Rev. Lett. **121**, no. 16, 162002 (2018).
- [18] J. Yelton *et al.* (Belle Collaboration), Phys. Rev. Lett. **121**, no. 5, 052003 (2018).
- [19] M. Sumihama *et al.* (Belle Collaboration), [arXiv:1810.06181 [hep-ex]].
- [20] D. Teodoro *et al.*, Phys. Lett. **77B**, 451 (1978).
- [21] S. F. Biagi *et al.*, Z. Phys. C **34**, 175 (1987).
- [22] Y. F. Wang, Int. J. Mod. Phys. A **21**, 5371 (2006).
- [23] M. Ablikim *et al.* (BESIII Collaboration), Nucl. Instrum. Meth. A **614**, 345 (2010).
- [24] S. Jadach, B. F. L. Ward and Z. Was, Comput. Phys. Commun. **130**, 260 (2000); S. Jadach, B. F. L. Ward and Z. Was, Phys. Rev. D **63**, 113009 (2001).
- [25] R. G. Ping *et al.*, Chin. Phys. C **32**, 599 (2008); D. J. Lange, Nucl. Instrum. Meth. A **462**, 152 (2001).
- [26] S. Agostinelli *et al.* (GEANT4 Collaboration), Nucl. Instrum. Meth. A **506**, 250 (2003); J. Allison *et al.*, IEEE Trans. Nucl. Sci. **53**, 270 (2006).
- [27] E. Kuraev and V. S. Fadin, Sov. J. Nucl. Phys. **41** (1985) 466.
- [28] Y. S. Zhu, Chin. Phys. C **32**, 363 (2008); G. D' Agostini, New Jersey, USA: World Scientific (2003) 329 p.
- [29] R. Baldini, S. Pacetti, A. Zallo and A. Zichichi, Eur. Phys. J. A **39**, 315 (2009).
- [30] A. B. Arbuzov and T. V. Kopylova, JHEP **1204**, 009 (2012).
- [31] A. Sommerfeld, Ann. Phys. **403**, 257 (1931).
- [32] A. D. Sakharov, Sov. Phys. Usp **34**, 375 (1991).
- [33] C. Tzara, Nucl. Phys. B **18**, 246 (1970).
- [34] M. Ablikim *et al.* (BESIII Collaboration), Chin. Phys. C **39**, no. 9, 093001 (2015).
- [35] M. Ablikim *et al.* (BESIII Collaboration), Phys. Rev. D **93**, no. 7, 072003 (2016); arXiv:1907.13041 [hep-ex].
- [36] M. Ablikim *et al.* (BESIII Collaboration), Phys. Rev. Lett. **118**, no. 9, 092001 (2017).
- [37] L. Maiani, V. Riquer, F. Piccinini and A. D. Polosa, Phys. Rev. D **72**, 031502 (2005); X. Liu, X. Q. Zeng and X. Q. Li, Phys. Rev. D **72**, 054023 (2005); S. L. Zhu, Phys. Lett. B **625**, 212 (2005).
- [38] F. E. Close and P. R. Page, Phys. Lett. B **628**, 215 (2005).

Supplemental Material

The \sqrt{s} is the e^+e^- CM energy [1], \mathcal{L} is the integrated luminosity of each data set updated measurement with the same method as Ref. [2], the vacuum polarization correction factor $|1 + \Pi|$, the ISR correction factor $1 + \delta$, the detection efficiency ϵ , the number of signal events (the number of signal events for the upper limit estimation) $N_{\text{obs}}(N_{\text{obs}}^{\text{UL}})$, the Born cross section σ^B , the effective form factor $|G_{\text{eff}}(s)|$ and statistical significances $S(\sigma)$ for 15 energy points are summarized in Table I, where the double counting effect for statistical uncertainties are taken into account based on MC simulation.

TABLE I. The $e^+e^- \rightarrow \Xi^-\bar{\Xi}^+$ cross section and effective form factor from 15 energy points. The first uncertainties are statistical, and the second ones are systematic uncertainties.

\sqrt{s} (GeV)	\mathcal{L} (pb^{-1})	$ 1 + \Pi $	$1 + \delta$	ϵ (%)	$N_{\text{obs}}(N_{\text{obs}}^{\text{UL}})$	σ^B (fb)	$ G_{\text{eff}}(s) \times 10^{-3}$	$S(\sigma)$
4.0076	482.0	1.05	0.95	29.74 ± 0.13	24.9 ± 5.9	$136.4 \pm 36.2 \pm 17.3$	$6.4 \pm 0.9 \pm 0.4$	4.0
4.1783	3189.0	1.05	1.06	26.80 ± 0.12	127.9 ± 14.2	$106.3 \pm 13.2 \pm 13.5$	$6.0 \pm 0.5 \pm 0.4$	10.0
4.1888	524.6	1.06	1.06	28.48 ± 0.12	10.2 ± 4.5 (<16.7)	$47.6 \pm 23.5 \pm 6.0$ (<89.3)	$4.0 \pm 1.0 \pm 0.3$ (<5.5)	2.0
4.1989	526.0	1.06	1.07	26.74 ± 0.12	15.5 ± 5.1	$76.8 \pm 28.3 \pm 9.8$	$5.1 \pm 1.0 \pm 0.3$	3.0
4.2092	518.0	1.06	1.07	26.60 ± 0.12	10.7 ± 5.1 (<18.3)	$53.6 \pm 28.6 \pm 6.8$ (<105.0)	$4.3 \pm 1.2 \pm 0.3$ (<6.0)	2.0
4.2187	514.6	1.06	1.07	26.34 ± 0.12	29.0 ± 5.4	$147.8 \pm 30.8 \pm 18.8$	$7.1 \pm 0.8 \pm 0.5$	5.0
4.2263	1056.4	1.06	1.08	26.24 ± 0.11	39.8 ± 7.7	$98.2 \pm 21.3 \pm 12.5$	$5.8 \pm 0.7 \pm 0.4$	4.5
4.2357	530.3	1.06	1.09	26.11 ± 0.11	13.8 ± 4.9	$67.6 \pm 26.9 \pm 8.6$	$4.9 \pm 1.0 \pm 0.3$	3.0
4.2438	538.1	1.06	1.09	25.84 ± 0.11	20.0 ± 4.5	$97.5 \pm 24.6 \pm 12.4$	$5.8 \pm 0.8 \pm 0.4$	4.0
4.2580	828.4	1.05	1.09	26.66 ± 0.11	22.3 ± 6.1	$69.1 \pm 21.2 \pm 8.8$	$4.9 \pm 0.8 \pm 0.3$	3.5
4.2668	531.1	1.05	1.10	25.44 ± 0.11	17.7 ± 5.3	$88.9 \pm 29.8 \pm 11.3$	$5.6 \pm 1.0 \pm 0.4$	3.0
4.2777	175.7	1.05	1.09	25.50 ± 0.11	5.0 ± 2.2 (<8.1)	$76.4 \pm 37.6 \pm 9.7$ (<141.7)	$5.2 \pm 1.3 \pm 0.3$ (<7.1)	2.0
4.3583	543.9	1.05	1.14	23.66 ± 0.10	14.0 ± 3.7	$71.7 \pm 21.1 \pm 9.0$	$5.2 \pm 0.8 \pm 0.3$	3.0
4.4156	1043.9	1.05	1.16	22.79 ± 0.10	17.3 ± 5.2	$46.8 \pm 15.7 \pm 6.0$	$4.3 \pm 0.8 \pm 0.3$	3.0
4.5995	586.9	1.05	1.26	20.50 ± 0.10	5.4 ± 3.9 (<10.1)	$26.6 \pm 21.5 \pm 3.4$ (<56.9)	$3.4 \pm 1.4 \pm 0.2$ (<5.0)	1.0

Assuming that one-photon exchange $e^+e^- \rightarrow \gamma^* \rightarrow B\bar{B}$ is the dominating process, then the differential cross section can be straight-forwardly parameterized in terms of electric and magnetic form factors G_E and G_M . These are assumed to be the continuous functions of the momentum transfer squared, $s = q^2$.

The differential cross section for the process $e^+e^- \rightarrow \gamma^* \rightarrow \Xi^-\bar{\Xi}^+$ is given [3] by

$$\frac{d\sigma^B(s)}{d\Omega} = \frac{\alpha^2\beta C}{4s} [|G_M(s)|^2(1 + \cos^2\theta) + \frac{1}{\tau}|G_E(s)|^2\sin^2\theta], \quad (1)$$

Integrating over the full solid angle for Eq. 1, we get

$$\sigma^B(s) = \frac{4\pi\alpha^2 C\beta}{3s} [|G_M(s)|^2 + \frac{1}{2\tau}|G_E(s)|^2], \quad (2)$$

and then, we can define the effective form factor $G_{\text{eff}}(s)$ [4] with a linear combination of the electric and the magnetic form factor as

$$|G_{\text{eff}}(s)| = \sqrt{\frac{2\tau|G_M(s)|^2 + |G_E(s)|^2}{2\tau + 1}}. \quad (3)$$

From Eq. 2 and Eq. 3, the effective form factor can be further expressed by,

$$|G_{\text{eff}}(s)| = \sqrt{\frac{\sigma^B(s)}{(1 + \frac{1}{2\tau}) \cdot (\frac{4\pi\alpha^2 C\beta}{3s})}} = \sqrt{\frac{3s\sigma^B}{4\pi\alpha^2 C\beta(1 + \frac{2m_{\Xi}^2}{s})}} = \sqrt{\frac{4.48 \times 10^3 \sigma^B}{\frac{C}{s} \sqrt{1 - \frac{6.988 GeV^2}{s}} (1 + \frac{3.49 GeV^2}{s})}}, \quad (4)$$

the error of $|G_{\text{eff}}(s)|$ can be propagated to be

$$\delta_{|G_{\text{eff}}(s)|} = \frac{1}{2} C' \sqrt{\frac{1}{\sigma^B}} \cdot \delta_{\sigma^B}, \quad (5)$$

where δ_{σ^B} is error of σ^B .

[1] M. Ablikim *et al.* (BESIII Collaboration), Chin. Phys. C **40**, no. 6, 063001 (2016).

- [2] M. Ablikim *et al.* (BESIII Collaboration), *Chin. Phys. C* **39**, no. 9, 093001 (2015)
- [3] R. Baldini, S. Pacetti, A. Zallo and A. Zichichi, *Eur. Phys. J. A* **39**, 315 (2009).
- [4] B. Aubert *et al.* (BaBar Collaboration), *Phys. Rev. D* **73**, 012005 (2006)